

Chemically Driven Self-Division in Protocells Models.

Pablo Zambrano¹, Xiaoyao Chen¹, Christine M. E. Kriebisch¹, Brigitte A. K. Kriebisch¹, Job Boekhoven^{1,*}

¹Department of Bioscience, Technical University of Munich, Lichtenbergstrasse 4, 85748 Garching, Germany.

KEYWORDS: self-division; chemically fueled self-assembly; protocells; fuel-driven.

ABSTRACT: Division is crucial for replication of biological compartments and by extension a fundamental aspect of life. Current studies highlight the importance of simple vesicular structures in prebiotic conditions, yet the mechanisms behind their self-division remain poorly understood. Recent research suggests that environmental factors can induce phase transitions in fatty acid-based protocells, leading to vesicle fission. However, the transduction role of chemical energy in facilitating vesicle division has been less explored. This study investigates a mechanism of vesicle self-division driven by chemical energy without complex molecular machinery. We demonstrate that simple vesicles can undergo division into smaller daughter vesicles upon exposure to a chemical fuel. Our findings reveal that the division mechanism is finely controlled by adjusting fuel concentration, offering valuable insights into primitive cellular dynamics. This process showcases the robustness of self-division across different fatty acids, retaining encapsulated materials during division and suggesting protocell-like behavior. These results underscore the potential for chemical energy to drive autonomous self-replication in protocell models, highlighting a plausible pathway for the emergence of life. Furthermore, this study contributes to the development of synthetic cells, enhancing our understanding of the minimal requirements for cellular life and providing a foundation for future research in synthetic biology and the origins of life.

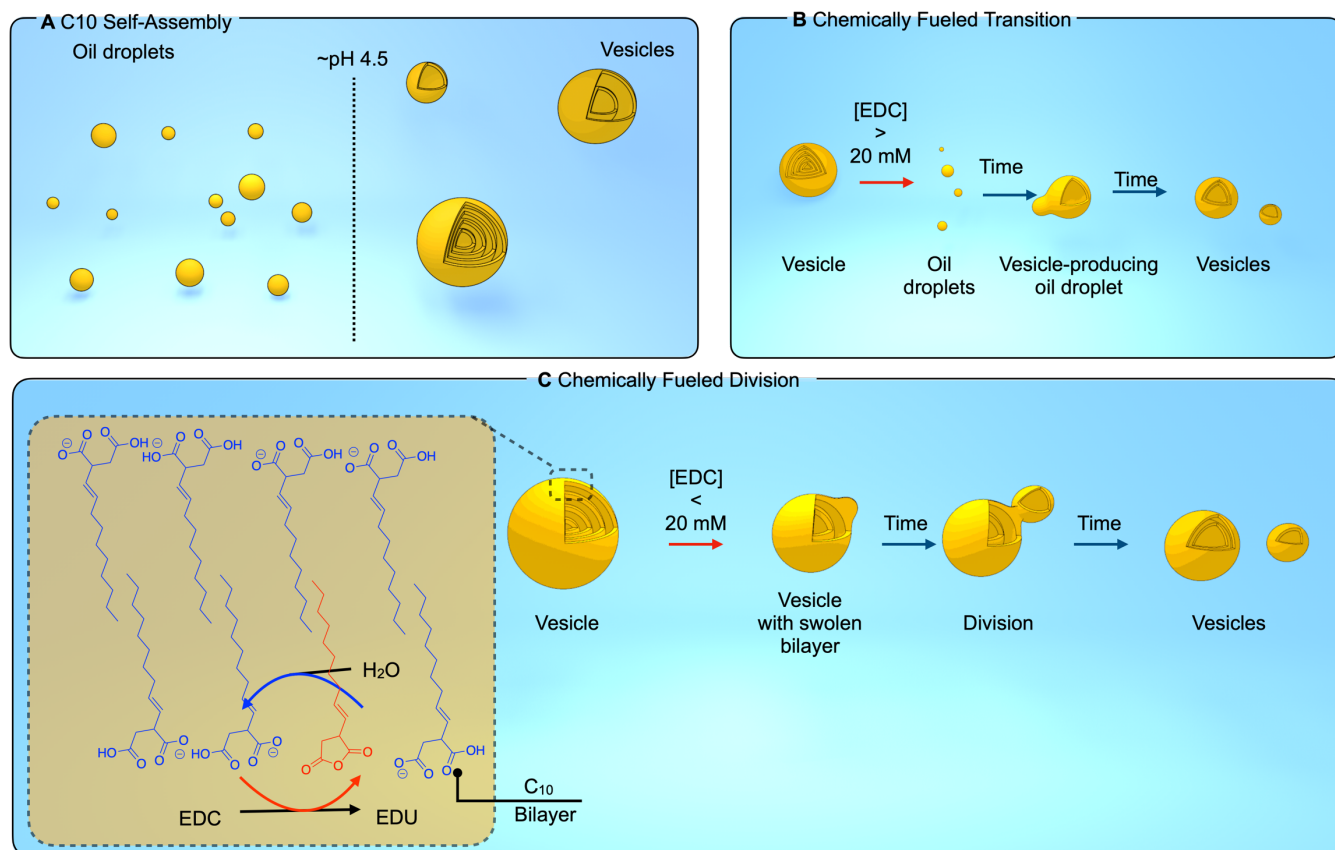
The essence of life depends fundamentally on the ability of biological compartments to replicate and divide, characteristics that are critical in all known life forms. The origins of life are thought to date back to simple structures, such as droplets or membranous vesicles composed of amphiphilic molecules, likely precursors of modern complex cellular architectures.¹⁻³ These primitive compartments, possibly formed by simple fatty acid vesicles, are fundamental to understanding how life could have begun under prebiotic conditions. Despite extensive studies, the mechanisms by which such simple vesicular structures could generate offspring through self-division, especially in the absence of the complex molecular machinery typical of contemporary life forms, remains poorly understood.⁴ In contrast, modern cell division within phospholipid compartments is highly regulated and involves intricate networks of macromolecular complexes, enzymes, and proteins.⁵ This process starkly contrasts early protocellular systems, which, lacking such complex components, must have relied on fundamentally different mechanisms for replication and division⁶⁻⁸.

The division of biological compartments that use chemical energy without the mediation of complex molecular machinery is rarely described, underscoring an important gap in our understanding of primitive life processes.⁹ Recent advances have highlighted how environmental factors such as temperature, pH, and UV light induce phase transitions in fatty acid-based protocells, leading to vesicle fission and daughter vesicles.^{4,7,10,11} These findings suggest that environmental conditions may have played a critical role in replicating early protocells. Furthermore, studies have shown that self-assembling single-chain amphiphiles, likely available in the prebiotic environment, played a fundamental role in the advent of primitive cell cycles.^{12,13} However, the instability of prebiotic fatty

acid-based membranes to temperature and pH suggests that primitive cells could only host prebiotically relevant processes in a narrow range of non-fluctuating environmental conditions.¹⁴

This work introduces a mechanism for membranous vesicle self-division facilitated by converting a sacrificial molecule with high chemical potential. We use a chemical cycle driven by a carbodiimide, a condensing agent hypothesized to have played a key role in prebiotic chemical reactions, to induce significant structural changes in vesicles composed of a succinic acid derivative.¹⁵⁻¹⁸ This highly versatile molecule can spontaneously form vesicles at pH above 4.5, while it exists as oil droplets at lower pH levels (Scheme 1a). The reaction cycle involves the conversion of the diacid-molecule within the vesicle into transient oily anhydride molecules (Scheme 1b,c), followed by rapid hydrolysis back to amphiphilic constituents. Interestingly, this dynamic process leads to the local formation of new bilayers and the generation of daughter vesicles. By carefully controlling the conversion, we can direct the formation of these vesicles, offering new insights into protocellular behaviors.

In addition, our research explores the transfer of molecular contents from progenitor vesicles to the newly formed compartments, providing insights into how protocellular systems might have managed resource distribution and compartmentalization during division. By elucidating this mechanism of chemically-driven self-division, our work aims to deepen our understanding of primitive cellular functions and contribute to the emerging field of synthetic biology, where creating cells with autonomous division capability remains a major challenge¹⁹⁻²¹. Finally, we extended our study of the self-dividing mechanism of our initial amphiphilic molecule to include prebiotic vesicles composed of decanoic acid, a molecule be



Scheme 1: Vesicle Formation and Self-Division Mechanism. (A) C10 forms oil droplets below pH 4.5 and vesicles above pH 4.5. (B) High EDC concentration converts vesicles to oil droplets, while low EDC induces vesicle division. (C) EDC facilitates the conversion to anhydride, leading to hydrolysis, bilayer formation, and daughter vesicle generation.

lied to have been abundant on the early Earth^{12,22–24}. Our results revealed that decanoic acid vesicles can divide even at low carbodiimide concentrations. This extension of our investigation demonstrates the robustness of the mechanism of self-division in different amphiphilic systems, suggesting that such processes could have played a crucial role in the self-replicative behaviors of early protocells. This aspect of our study not only tests the versatility of our proposed mechanism in diverse lipid-like environments but also enhances our understanding of the types of molecular assemblies that could have facilitated the emergence of life^{21,25}. Our work also lays the conceptual foundation for developing synthetic cells capable of autonomous self-replication, reflecting the most basic properties of life^{26,27}.

Results and Discussion

A Chemically Fueled Morphological Transition Towards Smaller Vesicles

For our amphiphiles, we use a succinic acid-based fatty acid. In previous work, we found that this molecule is readily converted to anhydride using chemical energy.¹⁶ Specifically, we used 2-decen-1-yl-succinic acid (C10) at 65 mM in 200 mM MES buffer, the condi-

tions throughout the work. We found that the behavior of C10 varies drastically with pH, which was investigated by confocal microscopy and turbidity measurements (Fig. S1)²⁸. At pH below 4.0, we observed that C10 predominantly forms oil droplets, whereas at pH above 4.5, unilamellar and multilamellar vesicles emerge clearly in solution. We measured the pK_a for C10 to be 5.41 (Fig. S2) and can therefore conclude that C10 transitions from vesicles to oil droplets when its carboxylates become protonated. This behavior is in line with other fatty acids that tend to form oil droplets at pH values below their pK_a and transition to form vesicles near their pK_a.^{12,29,30} Following our confocal microscopy findings, we focused on working at a pH of 4.9 to ensure a constant presence of vesicles. Additionally, we found that the critical vesicle concentration is above 1 mM (Fig S3). Additional confocal experiments were conducted to determine the optimal concentration of C10 at which vesicles were formed that were predominantly greater than 1 μm in size form (Fig S4-S6).

Our reaction cycle uses a condensing agent (1-ethyl-3-(3-dimethylaminopropyl)carbodiimide hydrochloride (EDC or fuel) as a chemical fuel to convert C10 to its corresponding

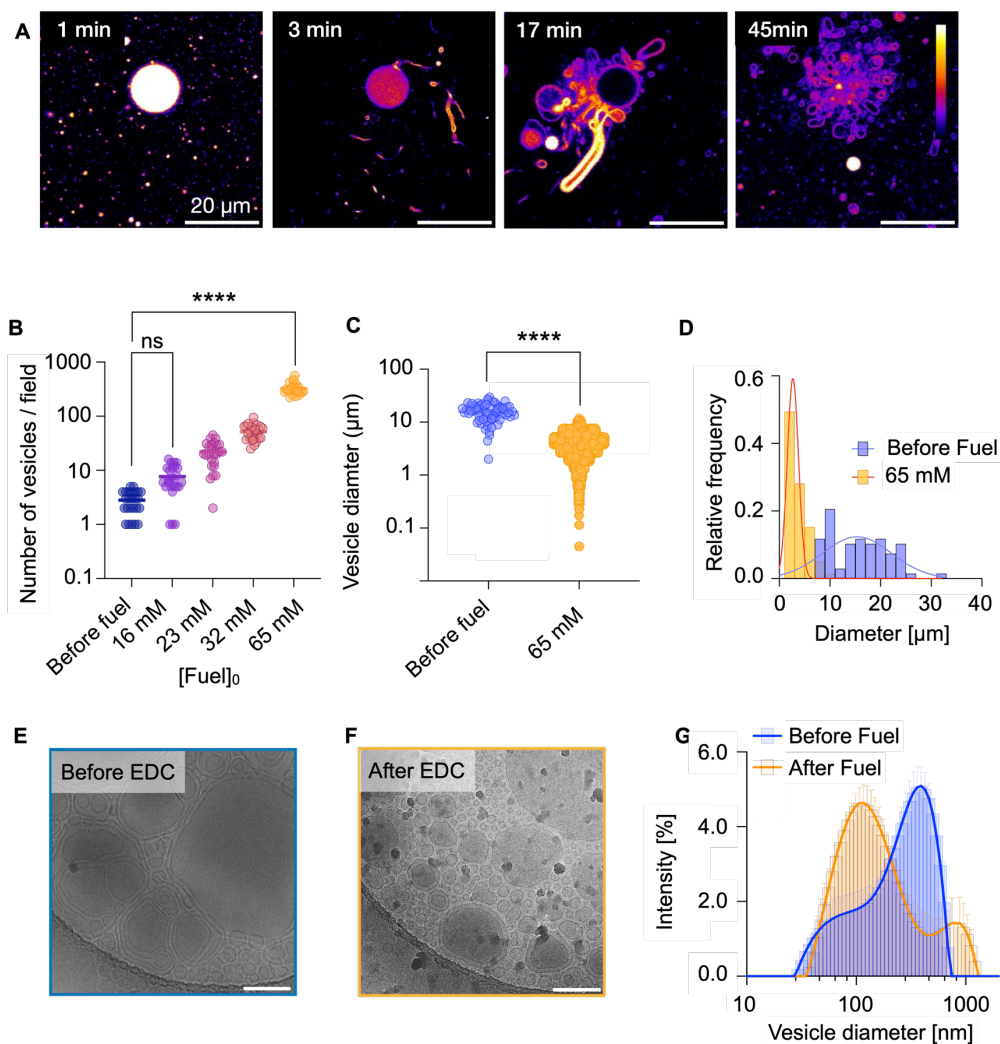


Figure 1. (A) Confocal micrographs of the morphological transition of a C10 multilamellar vesicle (65 mM) in response to EDC 23 mM at pH 4.9. The vesicles were stained with 2 μM Nile Red to highlight structural features. (B) The number of vesicles generated after adding different EDC concentrations. $n = 25$ (per condition, images analyzed). ANOVA was used to identify significant group differences, $p < 0.0001$ ****. Variance homogeneity was confirmed by Brown-Forsythe and Bartlett's tests, both $p < 0.0001$ ****. The model explains 91.92% of the variance ($R^2 = 0.9192$). (C) Average diameter of vesicles generated after addition of EDC 65 mM to C10 solution (65 mM). Unpaired t-test analysis between 'Before fuel' and 'EDC 65 mM', $p < 0.0001$ ****, $n = 68$ for 'Before fuel' and $n = 8131$ for 'EDC 65 mM'. (D) Comparative histogram and Gaussian fits of vesicle size distribution after addition of EDC 65 mM to C10 vesicles solution (65 mM). Bars represent vesicle size histograms for the 'Before fuel' group ($n = 68$, blue) and '65 mM EDC' group ($n = 8131$, orange). Lines represent Gaussian fits: 'Before fuel' group (blue): amplitude 0.1236, mean 15.36 μm , SD 6.820 μm ; '65 mM EDC' group (orange): amplitude 0.5916, mean 2.684 μm , SD 1.103 μm ; (E) cryo-TEM micrographs of C10 vesicles (65mM; MES buffer 200 mM; pH 4.9) before and after (F) addition of EDC 23 mM. Scale bar: 200 nm; (G) Results of dynamic light scattering (DLS) analysis of 400 nm multilamellar C10 vesicles obtained by extrusion (blue) after exposure to 23 mM EDC (orange). Error bars represent standard deviations (SD) with $n = 3$.

anhydride (activation). The anhydride is unstable in the aqueous medium and hydrolyzes to the precursor (deactivation). Therefore, when a finite amount of fuel is added, the anhydride emerges and disappears again as the fuel is depleted.^{15,17,18} Using confocal microscopy, we observed remarkable transformations upon adding EDC to a vesicle solution of 65 mM C10— in the first 60 seconds after adding 23 mM EDC, we observed a marked increase in the fluorescence intensity of the vesicles. This increase is attributed to the solvatochromic dye Nile Red, whose quantum yield is greater in oily phases than in lipid bilayers. Moreover, minutes after the addition of EDC, the lumen of the vesicles was no longer observed (Fig. 1A). We conclude that the vesicles were almost all completely converted to oil droplets as a result of the partial conversion of the C10 into its corresponding anhydride. In the following minutes, the

fluorescence intensity decreased again, and new membranous structures formed on the surface of the oil droplets. These new "daughter" vesicles were initially elongated and attached to the mother vesicle, then began to grow and, after 15 min, adopted unilamellar and multilamellar forms. However, these new vesicles remained attached to the mother vesicle until, finally, the original multilamellar vesicles reduced in size and disappeared completely, leaving a set of separate, individual daughter vesicles (Fig. 1A, Fig. S7, Movie S1-S2). Likely, the new vesicles formed as the reaction cycle was deactivating the anhydride state and thus, locally, producing C10 amphiphiles. In addition, we monitored the pH of the reaction cycle throughout the experimental timeline to ensure that pH fluctuations did not influence our observations. Consistently, the

pH remained stable at around 4.95 after adding EDC (Supplementary Table 3)

We quantified the production of daughter vesicles using confocal microscopy, by imaging the C10 vesicles before and after adding varying concentrations of EDC, with at least 25 images captured per condition. We observed that the number of vesicles increases significantly with higher EDC concentrations, evidencing a dramatic increase when the EDC concentration is raised from 16 mM to 65 mM (Fig. 1B). For example, with 16 mM EDC, the number of vesicles doubles compared to the initial amount observed before fuel addition. This upward trend suggests that the efficiency of EDC-induced vesicle division is markedly enhanced as its concentration increases. On the other hand, we also observed a significant reduction in the size of vesicles formed in response to EDC compared to the parent vesicles (Fig. 1C-D). Specifically, while the average diameter of the stock vesicles was approximately $15.8 \pm 5.6 \mu\text{m}$, the vesicles formed after EDC addition showed an average diameter of only $3.6 \pm 2.0 \mu\text{m}$ (Fig. S8). This demonstrates the efficacy of EDC in increasing the number of vesicles and its ability to promote structural cleavage of vesicles, resulting in smaller and more numerous units. This effect was more pronounced at higher EDC concentrations, where the decrease in vesicle size was even more evident. These changes reflect a dynamic process of vesicle reorganization and division driven by the addition of EDC.

To investigate whether this mechanism of EDC action depends on the initial vesicle size, we carried out experiments with C10 vesicles prepared by extrusion through a 400 nm filter. Before the addition of fuel, cryo-TEM micrographs reveal vesicles that were polydisperse in size ranging from a diameter of 50 nm to hundreds of nm, despite the extrusion at 400 nm (Fig. 1E). We hypothesize that the vesicles rapidly fuse due to their fatty acid nature and their high concentration. Furthermore, DLS confirmed the polydisperse nature with a broad peak centered around 400 nm (Fig. 1G). Nevertheless, 1.5 hours after adding 23 mM EDC, cryo-TEM micrographs show a marked decrease in vesicle size (Fig. 1F). DLS analysis further corroborates these observations—following the EDC exposure, the DLS data reveals a significant shift in the size distribution towards smaller vesicle sizes, around 100 nm. Additionally, a secondary peak around 1000 nm suggests the presence of larger vesicular structures pointing towards the rapid fusion of these vesicles. These findings generally align with recent studies suggesting membrane phase transitions driven by environmental fluctuations can generate daughter protocells with reorganized contents.^{4,10} In contrast to these studies, where phase transitions are induced by temperature and pH fluctuations, our research demonstrates that fuel-driven chemical conversion can effectively induce vesicle division and daughter vesicle formation.

Controlled Activation Leading to Vesicle Self-Division

The data above shows chemical fuel can induce a morphological transition from vesicles to oil droplets to smaller vesicles. However, the intermediate oil droplets are destroying the original vesicles, and the process is too drastic to call it self-division. We hypothesized that smaller amounts of fuel could prevent the complete collapse of the vesicles into oil droplets and, instead, lead to a bilayer swollen with some oil. The local production of fatty acids through

the oil's hydrolysis could produce new vesicles. Such a process would be closer to self-division. Following this approach, we added less fuel to the multilamellar vesicles (10 mM EDC, 65 mM C10, pH 4.9). Data obtained by confocal microscopy showed that activation of the precursor results in a moderate increase in fluorescence intensity of the vesicles surface, indicating a slower minor conversion of the precursor to anhydride (Fig. 2A; Movie S3). Importantly, the multilamellar vesicles mostly stayed intact instead of fully converting to an oil droplet. Surprisingly, after 8 min, we could observe the formation of thin, unilamellar membranous structures on the surface of the multilamellar vesicles, which slowly grew into elongated compartments (Fig. S9). These new membranous structures remained attached to the mother vesicle for more than 7 min until they finally separated from the mother vesicle. This process of producing daughter vesicles continued for 15 minutes. The division behavior was heterogeneous as some vesicles produced many small daughter vesicles, whereas others produced only a few. The heterogeneity is likely a result of localized variations in the concentration of reactants and the structural integrity of the vesicle membrane. Observing these varying growth rates provides valuable insights into the mechanistic aspects of vesicle division, highlighting the complex interplay between chemical kinetics and membrane dynamics (Fig. S9, Movie S4-S5).

To understand the chemical kinetics behind the self-division, we used high-performance liquid chromatography (HPLC) to examine the evolution of the concentrations using 65 mM C10 and 10 mM EDC. We monitored the concentration of C10, its corresponding anhydride, and EDC (Fig. 2B; Fig. S10). We found an initial rapid increase in the anhydride concentration simultaneously with a consumption of the EDC. After this initial increase, the anhydride concentration steadily decreased until it disappeared within 30 minutes. This linear decay can be explained by a self-protection mechanism that we previously documented.^{16,18} In this mechanism, the anhydride is encapsulated and isolated from water, leading to the hydrolysis to occur exclusively on the anhydride that remains in the aqueous medium, resulting in a linear decrease of the anhydride until all droplets have completely dissolved. Such a pattern establishes that the decomposition rate is directly linked to the solubility of the anhydride, which is constant. Using this self-protection model, we could accurately fit and predict the reaction kinetics described in our reaction cycle (Supplementary Information - Methods).

In parallel, we monitored the evolution of the optical density at 600 nm by absorbance measurements in response to various amounts of fuel (Fig. 2C). The data revealed a rapid, slight increase in turbidity during the first few minutes after 10 mM EDC addition which we attributed to a gradual decrease in turbidity as these droplets hydrolyzed and dissolved. Minutes after, the turbidity decreased back to the original level. The process correlates nicely with the behavior of the system. With 10 mM of EDC, the division was mostly visible by microscopy in the first 10 minutes, backed by the anhydride and turbidity decaying in the first 10 minutes. When more EDC was added, the turbidity increased strongly, indicating the formation of oil droplets in line with our earlier observations (Fig. 1.).

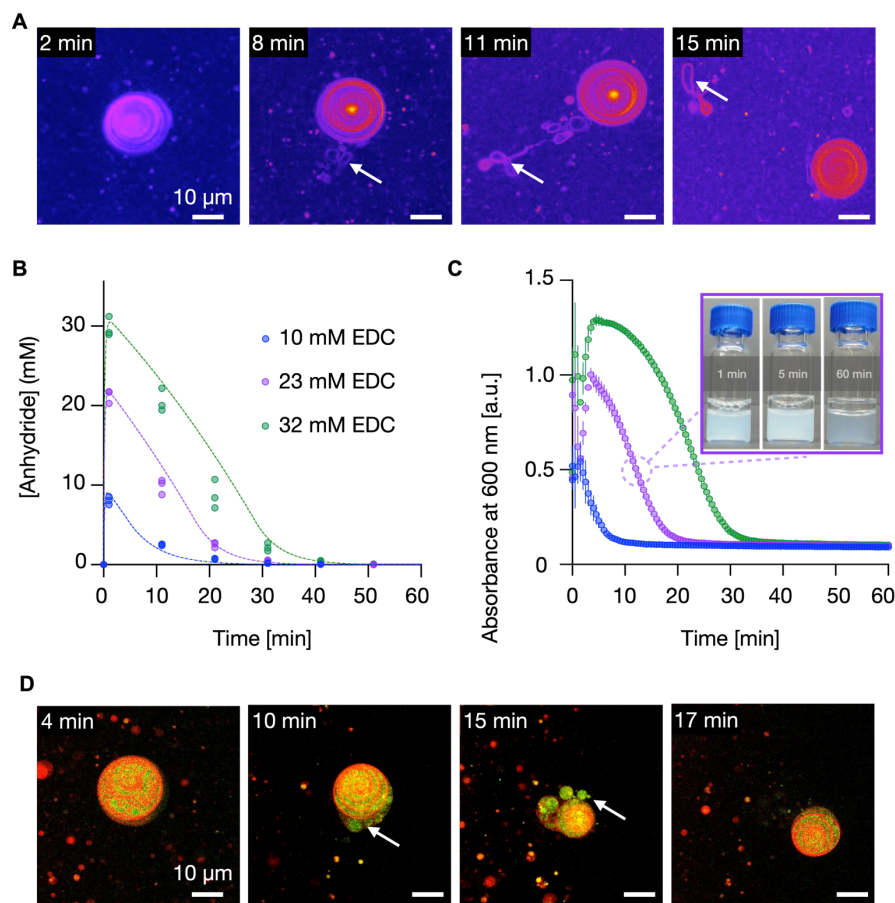


Figure 2. (A) Generation of "daughter" vesicles from the surface of a multilamellar vesicle. Conditions: C10 65 mM precursor (Nile Red dye; 2 μ M), EDC 10 mM, MES buffer 200 mM, pH 4.94. The arrow indicates the location of the emergence of the "daughter" vesicle and its trajectory until it detaches from the "mother" vesicle. (B) C10 anhydride concentration as a function of time (symbols; triplicates) and kinetic model (line) for 65 mM precursor in the presence of different EDC concentrations. (C) Turbidimetry measurements at 600 nm for 65 mM precursor at different EDC concentrations. Error bars represent standard deviations (SD) with $n = 3$. Inset: visual observation of turbidity changes over time. (D) Division process of multilamellar vesicles (labeled with 20 μ M Nile Red) with encapsulated material (labeled-DNA; 1.5 μ M) in the presence of 10 mM EDC. The sequence reveals the formation of smaller daughter vesicles, maintaining the integrity of the encapsulated material.

To refer to the production of new vesicles as a division, we ensured that the contents of the mother vesicles were transferred to the daughter vesicles instead of the production of new vesicles outside of the original one. Previous studies have shown that maintaining the integrity of encapsulated materials during vesicle division is a significant challenge, as many systems lose their internal contents due to membrane instability.^{6-8,13} Thus, we studied various techniques to encapsulate molecules within our multilamellar vesicles (See Supplementary Information – Methods) and found that they can retain fluorescently labeled DNA (Fig. S11). Remarkably, these vesicles managed to divide in response to 10 mM EDC and produced daughter vesicles smaller than the parent vesicle, which contained some of the encapsulated labeled DNA after the division. Confocal microscopy experiments (Fig. 2D; Movie S6) captured this process, where vesicles with Nile Red-stained membranes and encapsulated labeled DNA were observed at various time points

after adding 10 mM EDC. At 4 minutes, the vesicles showed partially converted anhydride membranes, indicated by a slight thickening. They increased Nile Red intensity compared to the thinner, intact vesicles (Fig. S11). By 10 minutes, small daughter vesicles began forming on the mother vesicle's surface, clearly retaining the encapsulated DNA within their interiors. By 15 minutes, these daughter vesicles slowly detached from the mother vesicle, as shown in the images. Finally, at 17 minutes, the mother vesicle was observed without the daughter vesicles, which had dispersed into the solution and moved out of the focal plane. We also found that EDC at the same concentration can induce inner membrane rearrangements in multilamellar vesicles (Fig. S12). This capacity to produce smaller daughter vesicles while preserving the encapsulated contents could have profound implications for developing synthetic cells and studying protocell evolution.

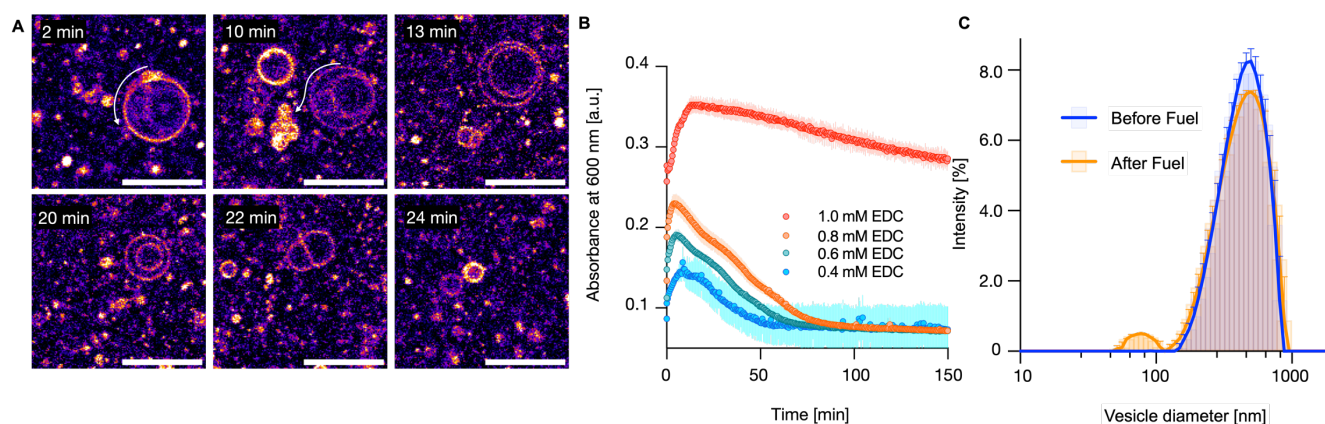


Figure 3. (A) Confocal micrographs showing the division sequence of decanoic acid (DA) vesicles (50 mM; pH 6.8) upon exposure to 0.4 mM EDC. Over time, the vesicle structure becomes disrupted, leading to the formation of smaller daughter vesicles. Dye: Nile Red 2 μM . Scale bar: 10 μm ; (B) Turbidimetry measurements at 600 nm for DA vesicles (50 mM) in MES buffer (200 mM, pH 6.8) with varying EDC concentrations (0.4–1.0 mM); (C) Dynamic light scattering (DLS) analysis of DA vesicles (400 nm multilamellar vesicles obtained by extrusion). The blue curve represents the size distribution of initial vesicles. In contrast, the orange curve shows the size distribution after exposure to 0.4 mM EDC (40 min). Error bars represent standard deviations (SD) with $n = 3$.

We extended our study to decanoic acid (DA), which is considered more prebiotically plausible than C10 and has been much more studied.^{22,24,31–33} First, we determined the critical concentration for vesicle formation (CVC) and the optimal pH for vesicle formation (Fig. S13-S16).^{4,12,23,34} At a concentration of 50 mM DA in 0.2 M MES buffer at pH 6.8, the vesicles were numerous and generally small, not exceeding 50 μm . Unlike the large multilamellar vesicles of C10, DA vesicles were predominantly unilamellar and more abundant (Fig. S16). We then investigated the behavior of these vesicles upon the addition of EDC (Fig. 3A). In line with the data on C10, at 2 minutes after 0.4 mM EDC addition, the Nile Red in the vesicle membrane exhibited increased brightness pointing to the intermolecular anhydride formation. Numerous smaller vesicles in the vicinity also transformed into anhydride droplets (bright points). Additionally, EDC induced an accumulation of anhydride in a specific region of the membrane (indicated by the arrow), which, after 10 minutes, hydrolyzed and formed smaller daughter vesicles. These daughter vesicles detached from the mother vesicle and dispersed into the solution (arrows). At 13 minutes, the mother vesicle underwent internal membrane reorganization, eventually leading to complete division by 24 minutes (Movie S7), demonstrating that the self-division mechanism explored with C10 also functioned effectively with decanoic acid. This finding is significant as it shows the robustness of the condensing agent-induced division mechanism across different amphiphilic systems.

In contrast to C10, much less EDC was required to induce a response by the system. For example, turbidimetry measurements at 600 nm with varying EDC concentrations show that as little as 0.4 mM EDC is sufficient to increase the turbidity (Fig. 3B) compared to the 10 mM EDC required to induce a response for C10 vesicles (Fig. 2B). We explain the drastic difference between the two seemingly similar amphiphiles by the drastically different nature of the anhydride. Specifically, we expect the anhydride of C10 to be drastically more water-soluble than its DA anhydride counterpart because the anhydride of C10 has an intramolecular anhydride, whereas the C10 anhydride is intermolecular. Therefore, the Carbon number per anhydride is almost twice as high for the anhydride

of DA, drastically decreasing solubility. As a result, less anhydride is needed to induce a response. In line with the C10 amphiphiles, the turbidity initially rose and leveled off over the course of an hour. Notably, the pH of the solution remained constant throughout the reaction, ensuring that the observed changes were due to the chemical processes induced by EDC rather than pH fluctuations (Table S4). Finally, we explored the reaction in nanometric DA vesicles obtained by extrusion (400 nm). Dynamic light scattering (DLS) analysis quantified the changes in size of these 400 nm multilamellar DA vesicles in the presence of EDC (Fig. 3C). After extrusion, the vesicles showed a relatively broad peak around 400 nm. One hour after the addition of EDC, the peak at 400 nm was still present but now accompanied by a smaller peak corresponding to vesicles of 50-100 nm in diameter, further corroborating the self-division of the fatty acid vesicles. The coherence between confocal microscopy, turbidimetry, and DLS data underscores the robustness of the chemical conversion mechanism in inducing vesicle division.

Conclusions

We demonstrated a fatty acid-based vesicle division mechanism driven by the chemical potential harvested from the hydration of the condensing agent EDC without relying on complex molecular machinery. Using vesicles comprising a succinic acid derivative (C10) or decanoic acid (DA), we observed that both systems, independently, could undergo division into smaller daughter vesicles even at low EDC concentrations. The DA vesicles also demonstrated self-division, supporting the robustness of this mechanism across different amphiphilic systems. This process retained encapsulated contents, suggesting potential protocell-like behavior. The findings indicate that the rate of anhydride hydrolysis and subsequent vesicle formation can be finely controlled by adjusting EDC concentration, offering valuable insights into the dynamics of primitive cellular processes. These insights contribute to the foundational understanding of developing synthetic cells capable of autonomous self-replication.

The ability of DA vesicles to undergo EDC-induced division without complete disintegration has significant implications for synthetic biology. This process provides a model for designing

robust, self-dividing synthetic cells that mimic early protocellular behaviors. Future research could focus on integrating genetic and metabolic components within these vesicles, advancing our understanding of the minimal requirements for cellular life. The insights gained from this study could inform the development of novel biomimetic materials and systems with applications in drug delivery, biosensing, and the creation of artificial life forms. This detailed analysis enhances our understanding of vesicle dynamics and division, opening new avenues for exploring the origins of life and developing synthetic biological systems.

Supporting Information

Extended materials and methods, supporting tables and figures with additional data and analysis, including rate constants, reaction pH over time, absorbance and titration curves, additional confocal micrographs, and supplementary movie descriptions.

Corresponding Author

* Prof. Dr. Job Boekhoven,
Department of Bioscience, Technical University of Munich, Lichtenbergstrasse 4, 85748 Garching, Germany.

Author Contributions

The manuscript was written through the contributions of all authors. All authors have approved the final version of the manuscript.

Acknowledgments: The BoekhovenLab is grateful for support from the TUM Innovation Network - RISE funded through the Excellence Strategy and the European Research Council (ERC starting grant 852187). This research was conducted within the Max Planck School Matter to Life, supported by the German Federal Ministry of Education and Research (BMBF) in collaboration with the Max Planck Society. This research was supported by the Excellence Cluster ORIGINS, funded by the Deutsche Forschungsgemeinschaft (DFG, German Research Foundation) under Germany's Excellence Strategy – EXC-2094 – 390783311. Cryo-TEM measurements were performed using the infrastructure the Dietz Lab and the TUM EM Core Facility contributed. P. Zambano thanks Dr. Oleksii Zozulia for the valuable discussions and Dr. Alexander Bergmann for the ideas provided at the beginning of this project.

References.

- (1) Deamer, D. The Role of Lipid Membranes in Life's Origin. *Life*. 2017. <https://doi.org/10.3390/life7010005>.
- (2) Segré, D.; Ben-Eli, D.; Deamer, D. W.; Lancet, D. The Lipid World. In *Origins of Life and Evolution of the Biosphere*; 2001; Vol. 31. <https://doi.org/10.1023/A:1006746807104>.
- (3) Hanczyc, M. M.; Monnard, P. A. Primordial Membranes: More than Simple Container Boundaries. *Current Opinion in Chemical Biology*. 2017. <https://doi.org/10.1016/j.cbpa.2017.07.009>.
- (4) Rubio-Sánchez, R.; O'Flaherty, D. K.; Wang, A.; Coscia, F.; Petris, G.; Di Michele, L.; Cicuta, P.; Bonfio, C. Thermally Driven Membrane Phase Transitions Enable Content Reshuffling in Primitive Cells. *J Am Chem Soc* 2021, 143 (40). <https://doi.org/10.1021/jacs.1c06595>.
- (5) Budin, I.; Szostak, J. W. Physical Effects Underlying the Transition from Primitive to Modern Cell Membranes. *Proc Natl Acad Sci U S A* 2011, 108 (13). <https://doi.org/10.1073/pnas.1100498108>.
- (6) Hanczyc, M. M.; Fujikawa, S. M.; Szostak, J. W. Experimental Models of Primitive Cellular Compartments: Encapsulation, Growth, and Division. *Science* (1979) 2003, 302 (5645). <https://doi.org/10.1126/science.1089904>.
- (7) Zhu, T. F.; Adamala, K.; Zhang, N.; Szostak, J. W. Photochemically Driven Redox Chemistry Induces Protocell Membrane Pearling and Division. *Proc Natl Acad Sci U S A* 2012, 109 (25). <https://doi.org/10.1073/pnas.1203212109>.
- (8) Zhu, T. F.; Szostak, J. W. Coupled Growth and Division of Model Protocell Membranes. *J Am Chem Soc* 2009, 131 (15). <https://doi.org/10.1021/ja900919c>.
- (9) Budin, I.; Szostak, J. W. Expanding Roles for Diverse Physical Phenomena during the Origin of Life. *Annual Review of Biophysics*. 2010. <https://doi.org/10.1146/annurev.biophys.050708.133753>.
- (10) Kudella, P. W.; Preißinger, K.; Morasch, M.; Dirscherl, C. F.; Braun, D.; Wixforth, A.; Westerhausen, C. Fission of Lipid-Vesicles by Membrane Phase Transitions in Thermal Convection. *Sci Rep* 2019, 9 (1). <https://doi.org/10.1038/s41598-019-55110-0>.
- (11) Attal, R.; Schwartz, L. Thermally Driven Fission of Protocells. *Biophys J* 2021, 120 (18). <https://doi.org/10.1016/j.bpj.2021.08.020>.
- (12) Jordan, S. F.; Ramm, H.; Zheludev, I. N.; Hartley, A. M.; Maréchal, A.; Lane, N. Promotion of Protocell Self-Assembly from Mixed Amphiphiles at the Origin of Life. *Nat Ecol Evol* 2019, 3 (12). <https://doi.org/10.1038/s41599-019-1015-y>.
- (13) Toparlak, D.; Wang, A.; Mansy, S. S. Population-Level Membrane Diversity Triggers Growth and Division of Protocells. *JACS Au* 2021, 1 (5). <https://doi.org/10.1021/jacsau.0c00079>.

- (14) Kundu, N.; Mondal, D.; Sarkar, N. Dynamics of the Vesicles Composed of Fatty Acids and Other Amphiphile Mixtures: Unveiling the Role of Fatty Acids as a Model Protocell Membrane. *Biophys Rev* 2020, 12 (5). <https://doi.org/10.1007/s12551-020-00753-x>.
- (15) Tena-Solsona, M.; Rieß, B.; Grötsch, R. K.; Löhrer, F. C.; Wanzke, C.; Käsdorf, B.; Bausch, A. R.; Müller-Buschbaum, P.; Lieleg, O.; Boekhoven, J. Non-Equilibrium Dissipative Supramolecular Materials with a Tunable Lifetime. *Nat Commun* 2017, 8. <https://doi.org/10.1038/ncomms15895>.
- (16) Schwarz, P. S.; Tebcharani, L.; Heger, J. E.; Müller-Buschbaum, P.; Boekhoven, J. Chemically Fueled Materials with a Self-Immolative Mechanism: Transient Materials with a Fast on/off Response. *Chem Sci* 2021, 12 (29). <https://doi.org/10.1039/d1sc02561a>.
- (17) Tena-Solsona, M.; Wanzke, C.; Riess, B.; Bausch, A. R.; Boekhoven, J. Self-Selection of Dissipative Assemblies Driven by Primitive Chemical Reaction Networks. *Nat Commun* 2018, 9 (1). <https://doi.org/10.1038/s41467-018-04488-y>.
- (18) Schwarz, P. S.; Tena-Solsona, M.; Dai, K.; Boekhoven, J. Carbodiimide-Fueled Catalytic Reaction Cycles to Regulate Supramolecular Processes. *Chemical Communications* 2022, 58 (9). <https://doi.org/10.1039/d1cc06428b>.
- (19) Xu, C.; Hu, S.; Chen, X. Artificial Cells: From Basic Science to Applications. *Materials Today*. 2016. <https://doi.org/10.1016/j.mattod.2016.02.020>.
- (20) Kurihara, K.; Okura, Y.; Matsuo, M.; Toyota, T.; Suzuki, K.; Sugawara, T. A Recursive Vesicle-Based Model Protocell with a Primitive Model Cell Cycle. *Nat Commun* 2015, 6. <https://doi.org/10.1038/ncomms9352>.
- (21) Dzieciol, A. J.; Mann, S. Designs for Life: Protocell Models in the Laboratory. *Chem Soc Rev* 2012, 41 (1). <https://doi.org/10.1039/c1cs15211d>.
- (22) Sepulveda, R. V.; Sbarbaro, C.; Opazo, M. C.; Duarte, Y.; González-Nilo, F.; Aguayo, D. Insights into Early Steps of Decanoic Acid Self-Assemblies under Prebiotic Temperatures Using Molecular Dynamics Simulations. *Membranes (Basel)* 2023, 13 (5). <https://doi.org/10.3390/membranes13050469>.
- (23) Jordan, S. F.; Nee, E.; Lane, N. Isoprenoids Enhance the Stability of Fatty Acid Membranes at the Emergence of Life Potentially Leading to an Early Lipid Divide. *Interface Focus* 2019, 9 (6). <https://doi.org/10.1098/rsfs.2019.0067>.
- (24) Namani, T.; Walde, P. From Decanoate Micelles to Decanoic Acid/Dodecylbenzenesulfonate Vesicles. *Langmuir* 2005, 21 (14). <https://doi.org/10.1021/la047028z>.
- (25) De Franceschi, N.; Barth, R.; Meindlhumer, S.; Fragasso, A.; Dekker, C. Dynamins A as a One-Component Division Machinery for Synthetic Cells. *Nat Nanotechnol* 2024, 19 (1), 70–76. <https://doi.org/10.1038/s41565-023-01510-3>.
- (26) Kurisu, M.; Imai, M. Concepts of a Synthetic Minimal Cell: Information Molecules, Metabolic Pathways, and Vesicle Reproduction. *Biophysics and physicobiology*. 2024. <https://doi.org/10.2142/biophysico.bppb-v21.0002>.
- (27) Insua, I.; Montenegro, J. Synthetic Supramolecular Systems in Life-like Materials and Protocell Models. *Chem*. 2020. <https://doi.org/10.1016/j.chempr.2020.06.005>.
- (28) Schnitter, F.; Bergmann, A. M.; Winkeljann, B.; Rodon Fores, J.; Lieleg, O.; Boekhoven, J. Synthesis and Characterization of Chemically Fueled Supramolecular Materials Driven by Carbodiimide-Based Fuels. *Nature Protocols*. 2021. <https://doi.org/10.1038/s41596-021-00563-9>.
- (29) Chen, I. A.; Walde, P. From Self-Assembled Vesicles to Protocells. *Cold Spring Harbor perspectives in biology*. 2010. <https://doi.org/10.1101/cshperspect.a002170>.
- (30) Morigaki, K.; Walde, P. Fatty Acid Vesicles. *Current Opinion in Colloid and Interface Science*. 2007. <https://doi.org/10.1016/j.cocis.2007.05.005>.
- (31) Todd, Z. R.; Cohen, Z. R.; Catling, D. C.; Keller, S. L.; Black, R. A. Growth of Prebiotically Plausible Fatty Acid Vesicles Proceeds in the Presence of Prebiotic Amino Acids, Dipeptides, Sugars, and Nucleic Acid Components. *Langmuir* 2022, 38 (49). <https://doi.org/10.1021/acs.langmuir.2c02118>.
- (32) Cohen, Z. R.; Todd, Z. R.; Wogan, N.; Black, R. A.; Keller, S. L.; Catling, D. C. Plausible Sources of Membrane-Forming Fatty Acids on the Early Earth: A Review of the Literature and an Estimation of Amounts. *ACS Earth and Space Chemistry*. 2023.

<https://doi.org/10.1021/acsearthspacechem.2c00168>.

- (33) Preiner, M.; Asche, S.; Becker, S.; Betts, H. C.; Boniface, A.; Camprubi, E.; Chandru, K.; Erastova, V.; Garg, S. G.; Khawaja, N.; Kostyrka, G.; Machné, R.; Moggioli, G.; Muchowska, K. B.; Neukirchen, S.; Peter, B.; Pichlhöfer, E.; Radványi, Á.; Rossetto, D.; Salditt, A.; Schmelling, N. M.; Sousa, F. L.; Tria, F. D. K.; Vörös, D.; Xavier, J. C. The Future of Origin of Life Research: Bridging Decades-Old Divisions. *Life* 2020, Vol. 10, Page 20 2020, 10 (3), 20. <https://doi.org/10.3390/LIFE10030020>.
- (34) Bonfio, C.; Russell, D. A.; Green, N. J.; Mariani, A.; Sutherland, J. D. Activation Chemistry Drives the Emergence of Functionalised Protocells. *Chem Sci* 2020, 11 (39). <https://doi.org/10.1039/d0sc04506c>.